

Neuroprotective effects of fecal microbiota transplantation on MPTP-induced Parkinson's disease mice: Gut microbiota, glial reaction and TLR4/TNF- α signaling pathway



Meng-Fei Sun¹, Ying-Li Zhu¹, Zhi-Lan Zhou, Xue-Bing Jia, Yi-Da Xu, Qin Yang, Chun Cui, Yan-Qin Shen*

Wuxi Medical School, Jiangnan University, Wuxi 214122, China

ARTICLE INFO

Article history:

Received 26 October 2017
Received in revised form 14 January 2018
Accepted 12 February 2018
Available online 20 February 2018

Keywords:

Parkinson's disease
Microbial dysbiosis
Gut-brain axis
Short-chain fatty acids
Glia
Neuroinflammation
Neurotransmitter
TLR4/TNF- α signaling

ABSTRACT

Parkinson's disease (PD) patients display alterations in gut microbiota composition. However, mechanism between gut microbial dysbiosis and pathogenesis of PD remains unexplored, and no recognized therapies are available to halt or slow progression of PD. Here we identified that gut microbiota from PD mice induced motor impairment and striatal neurotransmitter decrease on normal mice. Sequencing of 16S rRNA revealed that phylum *Firmicutes* and order *Clostridiales* decreased, while phylum *Proteobacteria*, order *Turicibacterales* and *Enterobacteriales* increased in fecal samples of PD mice, along with increased fecal short-chain fatty acids (SCFAs). Remarkably, fecal microbiota transplantation (FMT) reduced gut microbial dysbiosis, decreased fecal SCFAs, alleviated physical impairment, and increased striatal DA and 5-HT content of PD mice. Further, FMT reduced the activation of microglia and astrocytes in the substantia nigra, and reduced expression of TLR4/TNF- α signaling pathway components in gut and brain. Our study demonstrates that gut microbial dysbiosis is involved in PD pathogenesis, and FMT can protect PD mice by suppressing neuroinflammation and reducing TLR4/TNF- α signaling.

© 2018 Elsevier Inc. All rights reserved.

1. Introduction

Parkinson's disease (PD) is the second most common neurodegenerative disorder clinically characterized by motor and non-motor symptoms. The classical motor symptoms include bradykinesia, resting tremor, rigidity and late postural instability, due to progressive death of dopaminergic neurons in the substantia nigra pars compacta (SNpc) (Jankovic, 2008). However, there is also a wide spectrum of non-motor manifestations involving gastrointestinal (GI) dysfunction, such as dysphagia, constipation and weight loss, which occur frequently in PD and may precede motor symptoms (Goldstein et al., 2011; Kim and Sung, 2015). The emerging role of gut microbiota in GI pathogenesis and bidirectional communication between the gut and brain in PD has received much attention. Growing evidence shows that alterations in gut microbiota composition and microbial metabolites may be involved in the pathogenesis and clinical phenotype of PD (Scheperjans et al., 2015; Unger et al., 2016). For example,

PD patients showing a significant reduction of *Prevotellaceae* in their feces, as compared to normal individuals. Moreover, a direct correlation between the abundance of *Enterobacteriaceae* and severity of postural instability and gait difficulty has been found in PD patients (Scheperjans et al., 2015). Another study also demonstrated that the colonic bacterial phylum *Bacteroidetes* and the bacterial family *Prevotellaceae* were reduced while *Enterobacteriaceae* were more abundant in PD patients (Keshavarzian et al., 2015). Interestingly, gut microbiota from PD mice overexpressing α -synuclein (α -Syn) is required for motor deficits, microglia activation and α -Syn pathology, and germ-free mice receiving fecal microbiota transplantation (FMT) from PD patients display increased motor dysfunction (Sampson et al., 2016). However, the evidence for gut microbial dysbiosis in animals is lacking, and how gut microbial dysbiosis contributes to PD pathogenesis remains unknown. Similar to PD patients (Petrov et al., 2017; Scheperjans et al., 2015), we found that PD mice also display gut microbial dysbiosis, based on 16S rRNA sequencing. Remarkably, fecal samples from PD mice exhibit manifestations of gut microbial dysbiosis specifically with decreases in the phylum *Firmicutes* and order *Clostridiales*, and increases in the phylum *Proteobacteria*, order *Turicibacterales* and *Enterobacteriales*.

* Corresponding author at: Center for Neuroscience, Medical School of Jiangnan University, China.

E-mail address: shenyanqin@jiangnan.edu.cn (Y.-Q. Shen).

¹ These authors contributed equally.

To clarify the role of gut microbial dysbiosis in PD pathogenesis, we used a microbiota-targeted technique, named FMT, whereby infusion of feces (the entire gut microbiota) was delivered into the GI tract with gut microbial dysbiosis to re-establish a normal gut microbial community (Khoruts and Weingarden, 2014). Based on gut microbial dysbiosis, FMT is now applied for the treatment of autism, multiple sclerosis and other CNS diseases, possibly to regulate immunological mechanisms via the microbiota-gut-brain axis (Evrensel and Ceylan, 2016). Thus, we hypothesize that gut microbial dysbiosis contributes to the pathogenesis of PD, and that FMT may correct the gut microbial dysbiosis in PD. Given the evidence that gut microbiota contributes to microglial maturation and activation (Heijtza et al., 2011; Wang and Kasper, 2014), and microglial-induced neuroinflammation is thought to be one of the most important contributors to the pathogenesis of PD (Ransohoff, 2016), gut microbial dysbiosis may contribute to neuroinflammation. In fact, healthy intestinal epithelial cells express relatively low levels of Toll-like receptor 4 (TLR4) (Abreu et al., 2001), whereas gut microbial dysbiosis can lead to damage of the intestinal epithelial barrier and prompt activation of the TLR4/TNF- α signaling pathway, while TNF- α and some pro-inflammatory factors are not only able to induce peripheral immune activation and even cross the blood brain barrier to cause neuroinflammation in CNS under pathological conditions (Cani et al., 2008; Qin et al., 2007). Hence, we hypothesize that gut microbial dysbiosis regulates gut inflammation and neuroinflammation in PD via the TLR4/TNF- α pathway, and therefore FMT exert neuroprotection by suppressing the TLR4/TNF- α pathway via the microbiota-gut-brain axis.

Herein, we demonstrated that administration of fecal matter, from PD mice, caused wild-type C57BL/6 mice to display impaired motor function and decreased striatal dopamine (DA) and serotonin (5-HT) levels. We further demonstrated the neuroprotective effects of FMT administration in PD mice. Remarkably, FMT improved gut microbial dysbiosis, and decreased the activation of brain microglia and astrocytes, as well as lowered fecal concentrations of short-chain fatty acids (SCFAs) in PD mice. Further, FMT inhibited the TLR4/TBK1/NF- κ B/TNF- α signaling pathway-mediated gut inflammation and neuroinflammation, and rescued the levels of DA and 5-HT in PD mice.

Together, these results suggest us that gut microbial dysbiosis may play a critical and functional role in the pathogenesis of PD, impacting the balance of gut microbiota and SCFAs, motor functions. In addition, gut inflammation may influence brain functions by mediating the TLR4/TBK1/NF- κ B/TNF- α signaling pathway. Interestingly, FMT may protect PD mice by suppressing neuroinflammation and gut inflammation by reducing TLR4/TNF- α signaling.

2. Methods

2.1. Animals and group design

Eight-week-old male C57BL/6 mice (18 ± 2 g) were acquired from the Zhaoyan New Drug Research Center (Suzhou, China). The animals were maintained (5 mice/cage, 12 h light/dark cycle) under pathogen-free conditions in temperature (24 ± 2.0 °C) and humidity ($55 \pm 10\%$), and allowed access to food and water *ad libitum*. The food supplied for animal mice was commercial chow for SPF mice and rats (Jiangsu Xietong Organism, China). All experimental procedures were approved by the Animal Ethics Committee of Jiangnan University.

To verify the neuroprotection of FMT on PD mice, all animals were randomly divided into three groups: the normal control ($n = 15$ mice) without any treatment; the MPTP + PBS group ($n = 15$

mice), which was treated with 1-methyl-4-phenyl-1,2,3,6-tetrahydropyridine (MPTP) (Sigma-Aldrich) by intraperitoneal (*i.p.*) injection (30 mg/kg) for 5 days then PBS containing 20% sterile glycerol (200 μ l per mouse) by gavage for 7 days; and the MPTP + FMT group ($n = 15$ mice), which was treated with MPTP by *i.p.* injection for 5 days, then followed by FMT treatment (fecal microbiota from normal control mice) for 7 days.

In addition, to test the hypothesis that gut microbial dysbiosis is necessary to promote PD pathology, we designed the “NS + PD-FMT” group ($n = 10$ mice) which was treated with sterile normal saline (NS) for 5 days by *i.p.* injection, then followed by PD-FMT treatment (fecal microbiota from PD mice) for 7 days. Besides, two groups were designed to assess the potential effects of solvent and FMT, which named NS + PBS group ($n = 10$ mice) and NS + FMT group ($n = 10$ mice). The NS + PBS group mice got NS by *i.p.* for 5 days then PBS containing 20% sterile glycerol by gavage for 7 days, and the NS + FMT group mice got NS by *i.p.* for 5 days then FMT from normal mice for 7 days.

2.2. MPTP and FMT treatment

MPTP treatment: C57BL/6 mice received *i.p.* injections of MPTP (30 mg/kg) in a volume of 10 ml/kg of body weight once daily for 5 days. FMT treatment: Fresh fecal pellets were collected from PD mice or healthy control mice, then diluted immediately with sterile PBS (1 fecal pellet/ml). Briefly, the stool was steeped in sterile PBS for about 15 min, shaken and then centrifuged at 1000 rpm, 4 °C for 5 min. The suspension was centrifuged at 8000 rpm, 4 °C for 5 min to get total bacteria, then filtered twice in PBS. The final bacterial suspension was mixed with an equal volume of 40% sterile glycerol to a final concentration of 20%, then stored at -80 °C until transplantation (Hamilton et al., 2012). For each mouse, 200 μ l of bacterial suspension (10^8 CFU/ml) (Schuijt et al., 2016) was transplanted to each of the recipient mice by gavage each day for consecutive 7 days. The dilution coating method was used for determination of microbial concentrations from mice by calculating colonies on solid medium under anaerobic incubation as previously described (Ubeda et al., 2013).

2.3. Behavioral tests

On the 4th day of PBS or FMT treatment, the mice began behavioral training once per day for 3 days. The behavioral tests were performed on the first day after the last PBS or FMT treatment. Protocols of behavioral tests have been described in previous studies (Cao et al., 2017; Guo et al., 2015; Kuribara et al., 1977).

Pole descent test: a 0.5 m long pole, 1 cm in diameter and wrapped with non-adhesive gauze to facilitate gripping, and with a spherical protuberance, 2 cm in diameter on top, was placed in the home cage. Mice were placed head-down on the top of the pole and their descent back into the home cage was timed. Timing began when the experimenter released the animal and ended when one hind-limb reached the home cage base. The test was performed three times for each animal, beginning at the day after the last treatment, and the average time was taken.

Traction test: the forepaws of the mice were placed on a horizontal rope (diameter 5 mm) and observed for 10 s, while the hind limb placements were scored from 1 to 4, with the lowest score indicating the most severe deficit. Animals were assigned a score of 4 for gripping the rope with both hind paws, 3 for gripping the rope with one hind paw, 2 for gripping the rope with both front paws and 1 for gripping the rope with one front paw. The test was performed three times for each animal, beginning at the day after the last treatment, and the average score was taken.

2.4. Sample collection and tissue preparation

For collecting feces, normal control mice, MPTP-treated mice and FMT treated mice were placed individually in empty autoclaved cages and allowed to defecate freely in the morning after the day of last treatment. Once feces were formed of each mouse, they were collected immediately in individual sterile EP tubes on ice and then stored at -80°C until next usage.

For obtaining fresh striatum and colon tissue, mice were deeply anesthetized by isoflurane and then received a transcardiac perfusion of ice-cold sterilized saline (20 ml per mouse). The tissues were quickly dissected and immediately stored at -80°C . For immunofluorescence (IF), mice were transcardially perfused with PBS followed by 4% paraformaldehyde (PFA) in 0.01 M phosphate buffer, pH 7.4. Tissues were post-fixed in 4% PFA at 4°C overnight, kept in 20% sucrose at 4°C for 24 h, and next in 30% sucrose at 4°C for 24 h, and then embedded in optimal cutting temperature compound (O.C.T. Compound, Tissue-Tek, U.S.A.). Six micrometer-thick cross-sections were cut using a cryostat microtome (CM1950, Leica, Germany).

2.5. Gut microbiota profiling (DNA extraction and amplicon generation)

Fecal microbial genomic DNA was extracted using a FastDNA Spin Kit (Mbio, Carlsbad, USA), and the V4 regions of the 16S rRNA were amplified with primers (forward primer, 5'-AYTGGGYD TAAAGNG-3'; reverse primer, 5'-TACNVGGGTATCTAATCC-3') as described previously (Claesson et al., 2009; Klindworth et al., 2013; Zhang et al., 2017; Zhao et al., 2013). For amplification of the bacterial 16S rRNA gene V4 regions, the following PCR condition was used: 95°C for 3 min; then 30 cycles of 95°C for 30 s, 55°C for 30 s, 72°C for 30 s, and a final extension of 72°C for 5 min. The PCR products were purified with an AxyPrepDNA kit (AXYGEN, catalog No. AP-GX-50) and quantified by QuantiFlour-ST (Promega). Libraries were performed using a TruSeq DNA LT Sample Preparation Kit (Illumina, catalog No. FC-121-2001). An Illumina HiSeq 2500 was used to sequence the DNA to generate pair end 250 bp reads.

2.6. Bioinformatic analysis

Raw sequencing data was filtered according to the phred scores and the reads were trimmed if the average phred score in the window (5 bp in size, 1 bp step length) was <20 . The processed reads that were shorter than 150 bp were removed. After trimming, the reads were assembled by Flash software (Magoc and Salzberg, 2011), and the reads that could not be assembled were discarded. Then sequences that contained ambiguous bases, >1 mismatch in their 5' primers, or had a homopolymer over 8 or sequence length shorter than 200 bp were removed by Qiime (Caporaso et al., 2010). Only those high quality sequences without chimeras were used for further analysis. Uclust (Edgar, 2010) in Qiime was used to cluster the high quality sequences with a 97% similarity to obtain operational taxonomic units (OTUs). Then representative sequences of OTUs were annotated by comparing to the Greengenes database (13.5).

Weighted principal coordinate analysis (PCoA) was performed using UniFrac analysis (Lozupone and Knight, 2005) to represent the similarity among the microbial communities. Heatmap and PCoA were performed on R (version 3.0.3), while Venn diagrams were implemented by Venn Diagram software.

2.7. Fecal SCFAs analysis by gas chromatography-mass spectrometry (GC-MS)

Fresh fecal pellets were homogenized in sterile deionized water (1 mg feces/10 μl ddH₂O; 10%, w/v), then centrifuged at 13,000 rpm, 4°C for 5 min, to pellet the particulate matter. The supernatants were collected and filtered through a 0.22 μm filter, and 1 μl of sample was injected into the column. Quantitation of fecal SCFAs (acetic acid, propionic acid, butyric acid and n-valeric acid) was performed on a GCMS-QP2010 Ultra (Shimadzu Co., Tokyo, Shimadzu) fitted with an Rtx-WAX column (30 m \times 0.25 mm \times 0.25 μm , Bellefonte, PA, USA). The column was first kept at 100°C , and after 1 min, the column temperature escalated to 140°C at a rate of $7.5^{\circ}\text{C}/\text{min}$, and then to 230°C at $60^{\circ}\text{C}/\text{min}$. Helium was used as the carrier gas at a flow rate of 0.89 ml/min and the split ratio was 10:1. Temperatures of the injector, interface and ion source were 240, 250 and 220°C , respectively. The mass spectrometer was operated in selected ion monitor scan mode, and the selected ions for acetic acid, propionic acid, butyric acid and n-valeric acid were 43, 74, 60 and 60 m/z .

The external standard method was used to obtain the contents of target acids in samples. SCFAs mixtures consisting of the four acids were prepared at a series of concentrations of 5, 10, 20, 40, 60, 80 and 100 $\mu\text{g}/\text{ml}$ to construct the calibration curves. The calibration curve samples were treated in a similar way as the study samples.

2.8. Measurement of neurotransmitters and metabolites by high-performance liquid chromatography (HPLC)

Striatal DA, 5-HT and their metabolites, including dihydroxyphenylacetic acid (DOPAC), homovanillic acid (HVA) and 5-hydroxyindoleacetic acid (5-HIAA) were quantified by HPLC with a fluorescence detector (Waters 2475), following previous methods with some modifications (Ahmed et al., 2014). The separation system (Waters 2695, U.S.A.) was used with an Atlantis T3 column (150 mm \times 4.6 mm, 5 μm , Waters). The mobile phases were water, acetonitrile and 0.01 M phosphate buffer (adjusted to pH 4 with phosphoric acid), using gradient elution.

Briefly, the freshly isolated striatum was homogenized in 0.1 M perchloric acid (1mg:10 μl) and the homogenate was centrifuged at 13,000 rpm, 4°C for 10 min. Then, the supernatants were collected and filtered through a 0.22 μm filter and 25 μl of sample was injected into the column. In parallel, DA, 5-HT and their metabolites (DOPAC, HVA, 5-HIAA), and a hydrochloride standard (Sigma-Aldrich) solution were prepared freshly by diluting the stock solution in the mobile phase. The linearity range of DA was determined by serial concentrations of standard solution before detection.

2.9. Western blot analysis

Total protein was extracted by homogenizing 20 mg tissue in RIPA buffer (Beyotime, China) with 1% phenylmethanesulfonyl fluoride (PMSF) (Solarbio, China). After centrifugation of the homogenate at 13,000 rpm, 4°C for 5 min, protein concentration in the supernatant was determined with a BCA kit (Solarbio, China). The supernatant was denatured by boiling for 5 min in SDS sample buffer. 40 μg of total protein were separated by 6%–15% SDS-PAGE, blotted onto PVDF membranes, and then probed with the following antibodies: mouse anti-tyrosine hydroxylase (1:1000, MAB318, Millipore), rabbit anti-TLR4 (1:1000, 19811-1-AP, Proteintech), rabbit anti-NF- κB (1:1000, #8242, Cell Signaling Technology), rabbit anti-TBK1 (1:2000, ab40676, Abcam) and mouse anti-GAPDH

(1:1000, AF0006, Beyotime, China). Goat anti-rabbit IgG (1:1000, A0208, Beyotime, China) and goat anti-mouse IgG (1:1000, A0216, Beyotime, China) conjugated to horseradish peroxidase were used as secondary antibodies. Protein bands were visualized by incubation with BeyoECL Plus (P0018, Beyotime, China) for 1 min and imaged by a Gel Image System (Tanon, 5200, China). Densitometry was performed by using Image J software.

2.10. Enzyme-linked immunosorbent assay (ELISA)

TNF- α concentration of striatum and colon was detected using a commercial ELISA kit (Boster, EK0527, China). The limit of detection is 15.6–1000 pg/ml. All experimental procedures were performed according to the manufacturer's instructions. TNF- α concentration was expressed as pg/ml protein.

2.11. Immunofluorescence and image analysis

Briefly, each mouse brain was cut into coronal slices and slices containing the SNpc were collected. Brain sections were immersed in 0.01 M sodium citrate buffer (pH 6.0) for antigen retrieval and washed twice in PBS. Then, brain sections were incubated in PBS containing 0.2% v/v Triton X-100, 0.02% w/v sodium azide and 5% v/v goat serum for 1 h at 37 °C. Primary antibodies: mouse anti-tyrosine hydroxylase (1:1000, MAB318, Millipore), rabbit anti-GFAP (1:2000; Z033429, Dako, Denmark) and anti-Iba-1 (1:1000, 019-19741, Wako, Japan) were applied overnight at 4 °C. For detection of the primary antibodies, appropriate secondary antibodies, coupled to FITC-conjugated goat anti-mouse IgG (1:1000, A0568, Beyotime, China) or CY3-conjugated goat anti-rabbit IgG (1:1000, A0516, Beyotime, China) were used. Samples were covered with mounting medium (P0126, Beyotime, China) and examined with an epifluorescence microscope (Nikon eclipse 80i, Nikon, Japan).

For each animal, brain slices containing major part of SN from bregma -2.92 mm to -3.52 mm, 6 representative sections (space 100 μ m between) were chose to be doubly stained with tyrosine hydroxylase (TH) and Iba-1 or GFAP respectively. The cells positive for TH, Iba-1 and GFAP were counted in the right SN and the positive cells evaluation was used by the Image J analyzer (NIH, U.S.A.). The above-mentioned 6 representative sections were quantified for each animal, and each group contains 6 animals. These data are present as mean number of cells per section per group.

2.12. Statistical analysis

SPSS 22.0 software was used for data analysis. Statistical analysis was conducted by one-way ANOVA with an LSD post hoc assay. Data are presented as mean \pm s.e.m (standard error of the mean), and $P < 0.05$ was set as the threshold for significance ($*P < 0.05$, $**P < 0.01$, $***P < 0.001$). All data were displayed using Graph Pad Prism version 5.01 (Graph Pad, Inc, La Jolla, U.S.A.).

3. Results

3.1. FMT improves motor function of PD mice

Motor dysfunction commonly occurs in PD. To assess the potential neuroprotective effects of FMT on motor function in MPTP-induced PD mice, we subjected mice to a pole test to measure the total descent time for evaluation of bradykinesia, and a traction test to measure the traction score for evaluation of muscle strength and equilibrium. MPTP + PBS mice exhibited motor dysfunction, including longer pole descent time ($p < 0.001$ vs. normal controls) and lower scores in the traction test ($p < 0.001$ vs. normal controls) compared with normal control mice. However, FMT-recipient mice displayed significantly improved performance in pole descent test ($p < 0.001$ vs. the MPTP + PBS group) and traction test ($p < 0.001$ vs. the MPTP + PBS) compared with PBS treated mice (Fig. 1A and B). These results suggest that FMT improves the motor functions in PD model mice.

To assess the solvent effect and potential effects of gut microbiota from normal mice and PD mice on motor function in normal mice, pole descent test and traction test were also tested in NS + PBS group, NS + FMT group and NS + PD-FMT mice, MPTP + PBS group was set as PD model control. Total descent time was significantly longer in MPTP + PBS mice and NS + PD-FMT mice compared with NS + PBS mice and NS + FMT mice (Fig. S1A), respectively. Consistently, significant decrease in traction test score was observed in MPTP + PBS mice and NS + PD-FMT mice compared with NS + PBS mice and NS + FMT mice (Fig. S1B). There were no differences between NS + PBS group and NS + FMT group including pole descent test and traction test. These behavioral test results suggest that solvent or FMT has no effect on motor function of normal mice.

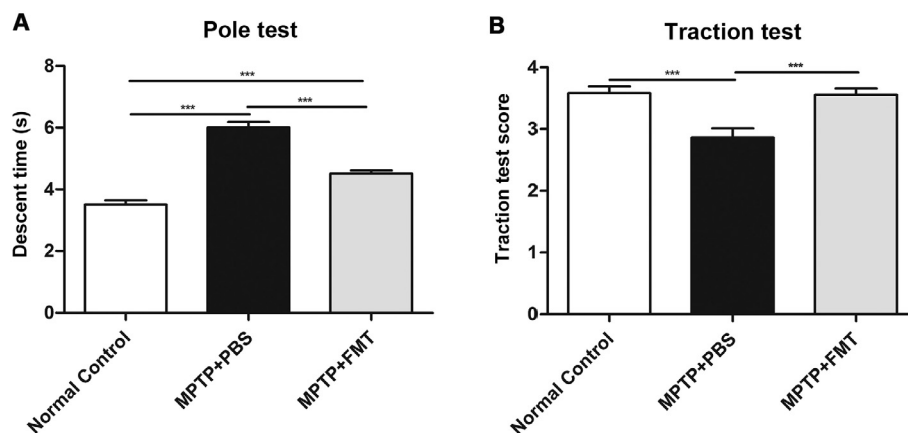


Fig. 1. FMT reduces motor dysfunction of PD mice while gut microbiota from PD mice promotes motor dysfunction of normal mice. (A) Pole descent test: time to descend the pole, as a measure of bradykinesia. Total descent time was significantly longer in MPTP + PBS mice compared with normal control mice, and shorter in MPTP + FMT mice compared with MPTP + PBS mice. (B) Traction test: traction reflex score for evaluation of muscle strength and equilibrium. The traction reflex score was significantly lower in and MPTP + PBS mice compared with normal control mice, and higher in MPTP + FMT mice compared with MPTP + PBS mice. Statistical comparison by one-way ANOVA with post hoc comparisons of LSD; Data represent the means \pm s.e.m; $***P < 0.001$. $n = 12$ mice per group.

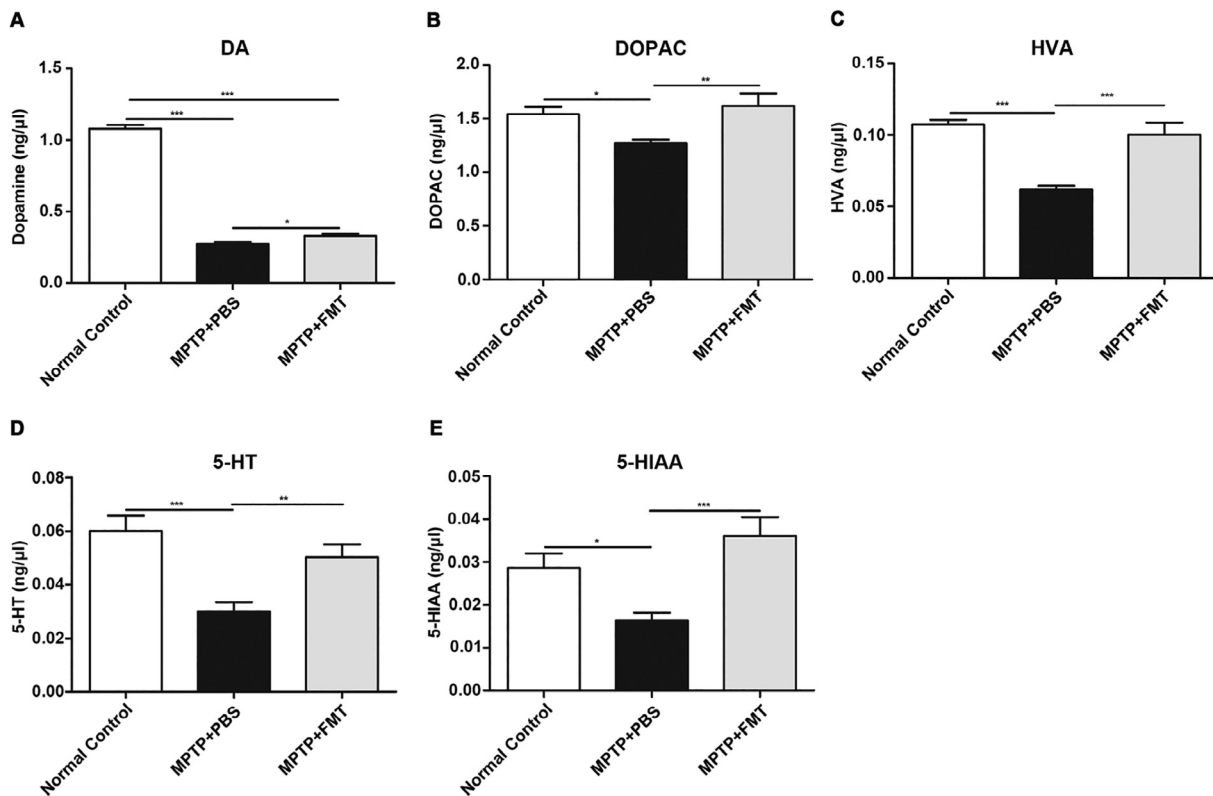


Fig. 2. FMT treatment of PD mice inhibits the MPTP-mediated reduction in brain neurotransmitters. (A) DA content in striatum shows higher DA expression in the MPTP + FMT group compared with the MPTP + PBS group. (B) DOPAC content in striatum shows the MPTP-mediated decrease of DOPAC expression was reversed by FMT. (C) HVA content in striatum shows the MPTP-mediated decrease of HVA expression was inhibited by FMT. (D) 5-HT content in striatum shows the MPTP-mediated decrease of 5-HT expression was inhibited by FMT. (E) 5-HIAA content in striatum shows the MPTP-mediated decrease of 5-HIAA expression was inhibited by FMT. DA, 5-HT and their metabolites were analyzed by HPLC. DA, 5-HT and their metabolites were analyzed by HPLC. Statistical comparison by one-way ANOVA with post hoc comparisons of LSD; Data represent the means \pm s.e.m.; * $P < 0.05$, ** $P < 0.01$, *** $P < 0.001$. $n = 8$ mice per group.

3.2. FMT rescued striatal dopamine and serotonin content of PD mice

To evaluate potential neuroprotective effects of FMT on brain function, the striatal neurotransmitters DA and 5-HT, and their metabolite (DOPAC, HVA and 5-HIAA) concentrations were measured by fluorescence detection following HPLC. As expected, striatal DA levels were dramatically decreased by 75.0% in MPTP + PBS mice compared with normal control mice ($p < 0.001$ vs. normal controls), but increased by 22.0% in MPTP + FMT mice compared to MPTP + PBS mice ($p < 0.05$ vs. MPTP + PBS group) (Fig. 2A). Similarly, DOPAC and HVA were also decreased by 17.5% and 45% in MPTP + PBS mice compared with control mice ($p < 0.05$ and $p < 0.001$ vs. normal controls, respectively). However, in MPTP + FMT mice, DOPAC and HVA were increased by 27.6% and 66.7% compared with the MPTP + PBS mice ($p < 0.01$ and $p < 0.001$ vs. MPTP + PBS group, respectively) (Fig. 2B and C). Similar to DA, 5-HT and its' metabolite 5-HIAA were also decreased by 50.0% and 44.8% in MPTP + PBS mice compared with normal control mice ($p < 0.001$ and $p < 0.05$ vs. normal controls, respectively), and a significant increase by 66.7% and 125% in MPTP + FMT mice compared with MPTP + PBS mice ($p < 0.01$ and $p < 0.001$ vs. MPTP + PBS group, respectively) (Fig. 2D and 2E). These results suggest that FMT participates in the metabolism of brain neurotransmitters by suppressing the MPTP-induced decline of striatal DA, 5-HT and their metabolites.

To assess the solvent effect and potential effects of gut microbiota from normal mice and PD mice on striatal neurotransmitters of normal mice, DA and 5-HT, and their metabolite (DOPAC, HVA and 5-HIAA) concentrations were also measured in NS + PBS group, NS + FMT group and NS + PD-FMT group, MPTP + PBS group was set as PD model control. Decreased DA levels (Fig. S2A), DOPAC

levels (Fig. S2B), HVA levels (Fig. S2C), 5-HT levels (Fig. S2D) and 5-HIAA levels (Fig. S2E) in MPTP + PBS and NS + PD-FMT group were found when compared with NS + PBS and NS + FMT groups respectively, and there were no differences between NS + PBS group and NS + FMT group. Clearly, solvent has no effect on striatal neurotransmitters of normal mice, and PD-FMT reduces neurotransmitters significantly in normal mice.

3.3. FMT restores dopaminergic neurons and TH levels in PD mice

To examine the effect of FMT on survival of dopaminergic neurons in the SN, and to verify whether TH expression corresponded with DA levels, we characterized TH expression by western blot analysis and IF staining in the SN. IF staining in the SN revealed a significant loss of TH+ dopaminergic neurons by 31.6% in MPTP + PBS mice compared to normal control mice ($p < 0.001$ vs. normal controls) that was partially rescued 32.6% by FMT ($p < 0.01$ vs. MPTP + PBS group) (Fig. 3A and B). Western blot analysis of striatal tissue showed that TH expression in MPTP + PBS mice was lower by 68.6% compared to normal control mice ($p < 0.01$ vs. normal controls), and FMT inhibited the reduction by 82.8% of TH expression in PD mice ($p < 0.05$ vs. the MPTP + PBS group) (Fig. 3C and D). These results demonstrate that the neuroprotective effects of FMT involve suppression of dopaminergic neuron loss in SN and decreased striatal TH expression in MPTP-induced PD mice.

3.4. Gut microbial dysbiosis in PD mice is reduced by FMT

To test our hypothesis that gut microbial dysbiosis also exists in PD mice (MPTP + PBS group) and FMT can improve the gut

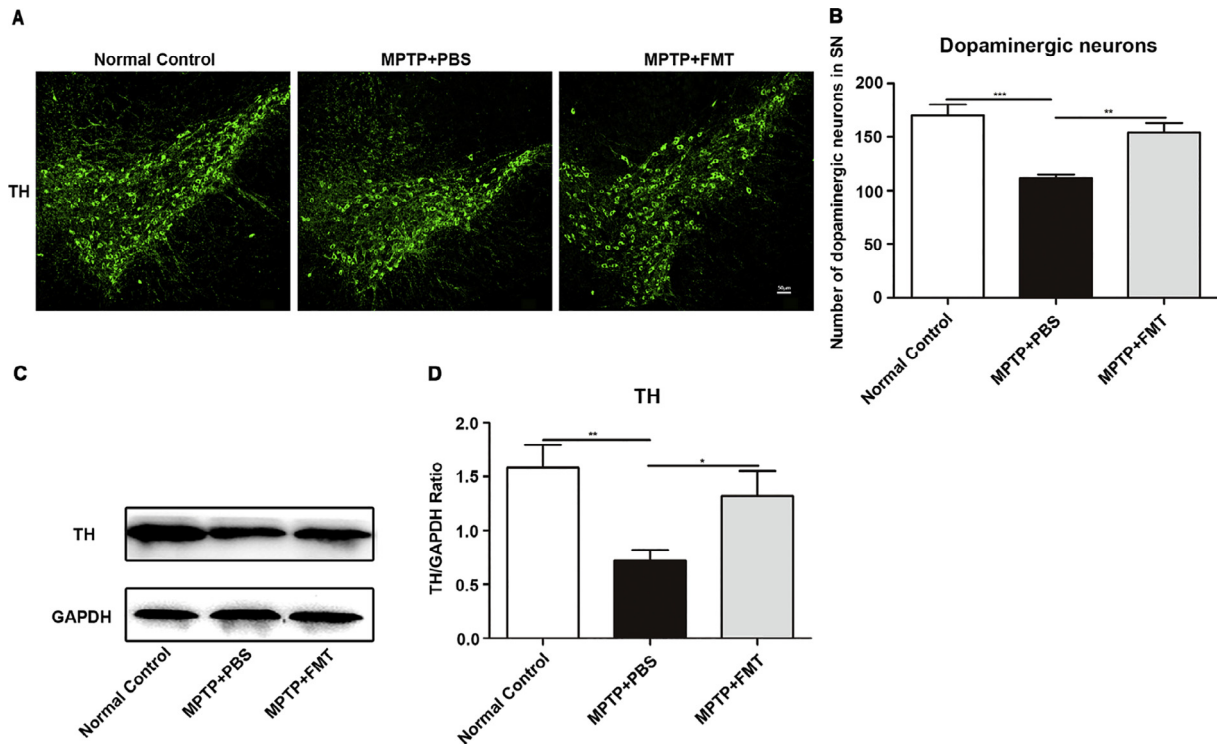


Fig. 3. FMT treatment of PD mice rescued the MPTP-mediated reduction in brain dopaminergic neurons and TH. (A) Representative IF staining for TH (dopaminergic neuron marker) in the SN. Scale bar is 50 μ m. (B) Quantitative analysis of the number of TH-positive cells in the SN. (C) Representative western blot of striatal TH expression. (D) The intensity of bands was quantified with Image J software and quantitative data for TH following normalization to GAPDH). Statistical comparison by one-way ANOVA with post hoc comparisons of LSD. Data represent the means \pm s.e.m.; * $P < 0.05$, ** $P < 0.01$, *** $P < 0.001$. $n = 6$ mice per group.

microbial dysbiosis in PD mice by affecting the microbiota composition, we performed relative analysis based on alpha and beta diversity measures, which provided a holistic view of gut microbiota and focus on abundance, diversity and distribution of gut microbiota. The alpha diversity indices of Chao1, representative of microbial diversity, tended to be higher in normal control (C) mice and MPTP + FMT (F) mice, compared to MPTP + PBS (M) mice (Fig. 4A), but there were no significant differences between the three groups, suggesting the number of samples need to be expanded. Beta diversity was further evaluated with UniFrac-based PCoA. Strikingly, using analysis of similarities (ANOSIM) of normal control, MPTP + PBS and MPTP + FMT groups, samples were clustered by subject ($p < 0.01$), indicating differences in microbial composition of PD mice, control mice and FMT-recipient mice (Fig. 4B). Also, other measures of alpha diversity indices including Shannon diversity and PD Whole tree was similar with Chao-1 (Fig. S3A and B). The differences in microbial communities between PD mice and normal mice suggested the presence of gut microbial dysbiosis in PD mice. To explore the abundance and distribution in gut microbiota in the three groups, and investigate the potential bacterial groups responsible for microbial dysbiosis, we identified a number of altered orders and phyla. Only those bacterial phyla and orders that averaged $>1\%$ of the relative abundance across all samples are displayed. The heatmap revealed a significant difference in relative abundance across the groups at the phylum level (Fig. 4C). A significant decrease was observed in the abundance of the phylum *Firmicutes* principally at the phylum level in MPTP + PBS mice compared to control mice. Interestingly, there were obvious increases in *Firmicutes* in FMT-recipient mice (Table 1). The abundance in phylum *Proteobacteria* was strikingly increased in MPTP + PBS mice compared to normal control mice, but comparatively lower in MPTP + FMT mice (Table 1). At the order level, the overall composition of gut microbiota was domi-

nated by the order *Clostridiales* (Fig. 4D). Decreased *Clostridiales* and increased *Turicibacterales* and *Enterobacteriales* were observed in PD mice compared to normal control mice, and FMT altered near the level of normal control (Table 2). Not only at the phylum and order level, significant difference of gut microbial was also obviously showed at genus level among three groups (Fig. S3C). Together, these data indicate that PD mice have gut microbial dysbiosis, and FMT can modulate the microbiota compositions to improve gut microbial dysbiosis in PD mice.

3.5. FMT alleviates glial-mediated neuroinflammation accompanied by restoration of normal SCFAs

Among the potential factors regulating the microbiota-gut-brain axis, microbial metabolites SCFAs may be the major mediators. We detected the fecal SCFAs concentrations in different groups (Table 3). Among fecal SCFAs (acetic acid, propionic acid, butyric acid and n-valeric acid) detected by GC-MS, acetic acid was changed most, which increased by 260.6% in MPTP + PBS mice compared with normal control mice. Interestingly, FMT decreased fecal acetic acid by 82.7% concentrations of PD mice (Fig. 5A). Propionic acid was also increased but changed least among four acids, which increased by 70.0% in MPTP + PBS mice compared with normal control mice. Instead, FMT decreased fecal propionic acid by 59.1% concentrations of PD mice (Fig. 5B). Similar to acetic acid, butyric acid and n-valeric acid were also increased in MPTP + PBS mice by 118.3% and 90.3% compared with normal control mice, while FMT significantly decreased fecal butyric acid and n-valeric acid by 72.0% and 65.4% concentrations of PD mice (Fig. 5C and D).

Given the evidence that SCFAs are sufficient to promote microglia-mediated neuroinflammation, based on morphology indicative of increased microglia activation (Sampson et al., 2016), we sought to determine whether brain glia are activated

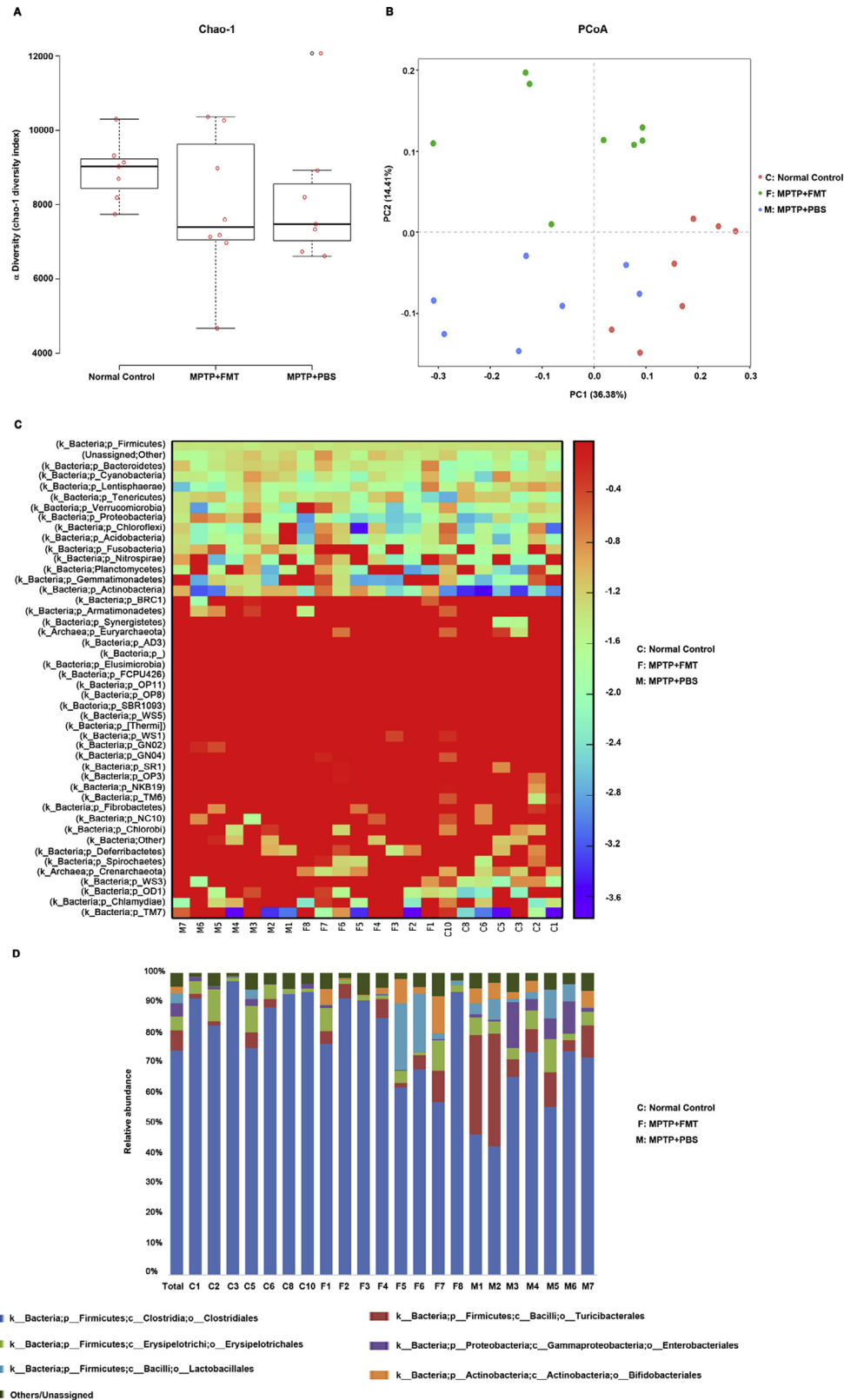


Fig. 4. Analysis of bacterial 16S rRNA from gut microbiota of PD mice shows FMT reduces PD microbial dysbiosis. (A) Analysis of alpha diversity-predicted diversity of gut microbiota by Chao-1 estimator analysis. (B) PCoA plots based on weighted UniFrac metrics of gut microbiota where samples of mice from different groups are highlighted with different colors. Principal components (PCs) 1 and 2 explain 36.38% and 14.41% of the variance, respectively. The position and distance of data points indicates the degree of similarity in terms of both the presence and relative abundance of bacterial taxonomies. (C) Heatmap based on the Bray-Curtis distance analysis about relative abundance of gut microbiota at the phylum level in three groups. (D) Distribution of relative abundance of gut microbiota at the order level observed in the three groups. Each color represents an order, and the height of the column represents the abundance of reads. Only those bacterial orders and phyla that comprised on average >1% of the relative abundance across all samples are displayed. “C” represents the normal control group, “M” represents the MPTP + PBS group, “F” represents the “MPTP + FMT” group. All other unassigned and classified OTUs belonging to phyla and orders comprising <1% of the total abundance are represented as Others/Unassigned. n = 7 mice in normal control and MPTP + PBS groups and n = 8 mice in MPTP + FMT group.

Table 1
Relative abundance of phyla >1% in different groups.

Phylum (relative abundance (%))	Group			P-value		
	Normal Control (C)	MPTP + PBS (M)	MPTP + FMT (F)	C vs. M	M vs. F	C vs. F
<i>Firmicutes</i>	95.53 ± 2.05	86.79 ± 4.96	91.54 ± 5.78	0.002**	0.062	0.112
<i>Proteobacteria</i>	1.31 ± 1.11	5.94 ± 5.64	0.45 ± 0.48	0.015*	0.004**	0.612
<i>Tenericutes</i>	1.99 ± 1.84	2.37 ± 1.25	2.15 ± 1.95	0.680	0.807	0.856
<i>Actinobacteria</i>	0.07 ± 0.08	3.10 ± 2.39	3.99 ± 4.50	0.078	0.58	0.022*
<i>Bacteroidetes</i>	0.41 ± 0.31	1.30 ± 0.48	1.36 ± 1.21	0.052	0.882	0.034*

Significant changes of phyla >1% present in different groups. "C" represents the normal control group (n = 7 mice), "M" represents the MPTP + PBS group (n = 7 mice), and "F" represents the "MPTP + FMT" group (n = 8 mice). Statistical comparison by one-way ANOVA with post hoc comparisons of LSD. Data represent the means ± SEM; *P < 0.05, **P < 0.01.

Table 2
Relative abundance of orders > 1% in different groups.

Order (relative abundance (%))	Group			P-value		
	Normal Control (C)	MPTP + PBS (M)	MPTP + FMT (F)	C vs. M	M vs. F	C vs. F
<i>Clostridiales</i>	88.83 ± 7.63	61.41 ± 13.22	78.14 ± 14.28	0.000***	0.016*	0.107
<i>Turicibacterales</i>	1.53 ± 1.91	15.66 ± 13.65	3.96 ± 3.49	0.004**	0.011*	0.565
<i>Erysipelotrichales</i>	4.64 ± 3.74	5.34 ± 2.87	3.69 ± 3.38	0.701	0.352	0.589
<i>Enterobacteriales</i>	0.94 ± 0.81	5.67 ± 5.57	0.23 ± 0.24	0.012*	0.004**	0.666
<i>Lactobacillales</i>	0.49 ± 1.15	4.19 ± 3.32	5.69 ± 9.38	0.265	0.636	0.112
<i>Bifidobacteriales</i>	0	3.07 ± 2.37	3.80 ± 4.41	0.07	0.643	0.024*
<i>RF39</i>	1.96 ± 1.8	1.46 ± 1.01	1.03 ± 1.95	0.579	0.620	0.533
<i>Bacteroidales</i>	0.37 ± 0.23	1.30 ± 0.48	1.36 ± 1.21	0.041*	0.880	0.026*

Significant changes of orders >1% present in different groups. "C" represents the normal control group (n = 7 mice), "M" represents the MPTP + PBS group (n = 7 mice), and "F" represents the "MPTP + FMT" group (n = 8 mice). Statistical comparison by one-way ANOVA with post hoc comparisons of LSD. Data represent the means ± SEM; *P < 0.05, **P < 0.01, ***P < 0.001.

Table 3
Fecal SCFAs contents in different groups.

SCFAs concentrations (ppm)	Group			P-value		
	Normal Control (C)	MPTP + PBS (M)	MPTP + FMT (F)	C vs. M	M vs. F	C vs. F
Acetic acid	65.96 ± 71.61	237.87 ± 94.46	41.27 ± 41.00	0.001**	0.000***	0.564
Propionic acid	30.68 ± 5.05	52.15 ± 27.30	21.34 ± 6.24	0.039*	0.005**	0.340
Butyric acid	25.15 ± 4.72	54.90 ± 39.73	15.37 ± 3.91	0.042*	0.010*	0.476
n-valeric acid	5.87 ± 0.89	11.17 ± 5.42	3.86 ± 0.48	0.011*	0.001**	0.290

Fecal SCFAs concentrations in different groups. "C" represents the normal control group, "M" represents the MPTP + PBS group, and "F" represents the "MPTP + FMT" group. Statistical comparison by one-way ANOVA with post hoc comparisons of LSD. Data represent the means ± SEM; *P < 0.05, **P < 0.01, ***P < 0.001. n = 6 mice per group.

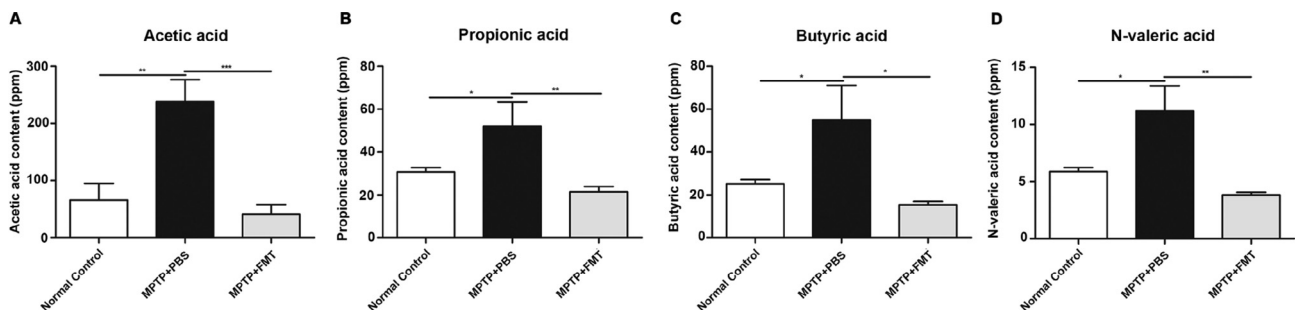


Fig. 5. Fecal SCFAs alterations in mice. (A) Fecal acetic acid content. The MPTP-mediated increase of acetic acid expression was inhibited by FMT. (B) Fecal propionic acid content. The MPTP-mediated increase of propionic acid expression was inhibited by FMT. (C) Fecal butyric acid content. The MPTP-mediated increase of butyric acid expression was inhibited by FMT. (D) Fecal n-valeric acid content. The MPTP-mediated increase of n-valeric acid expression was inhibited by FMT. SCFAs were analyzed by GC-MS. Statistical comparison by one-way ANOVA with post hoc comparisons of LSD. Data represent the means ± s.e.m; *P < 0.05, **P < 0.01, ***P < 0.001. n = 6 mice per group.

when fecal SCFAs increase abnormally. Thus, we measured the interactional activities between dopaminergic neurons and brain glia, including microglia and astrocytes, in the SN by IF staining. Double IF staining for TH (dopaminergic neuron marker) and GFAP (astrocyte marker) revealed the presence of a higher number of activated astrocytes by 91.4% in MPTP + PBS mice compared with normal control mice ($P < 0.001$ vs. normal controls), and FMT

significantly decreased the number of activated astrocytes around dopaminergic neurons by 37.3% on MPTP + PBS mice ($p < 0.001$ vs. the MPTP + PBS group) (Fig. 6A and B). Similarly, co-expression of TH with Iba-1 (marker for microglia) showed that, along with the loss of TH₊ neurons, more microglia in the SN were activated by 125.8% in MPTP + PBS mice compared with control mice ($p < 0.001$ vs. the normal controls), but in the MPTP + FMT group,

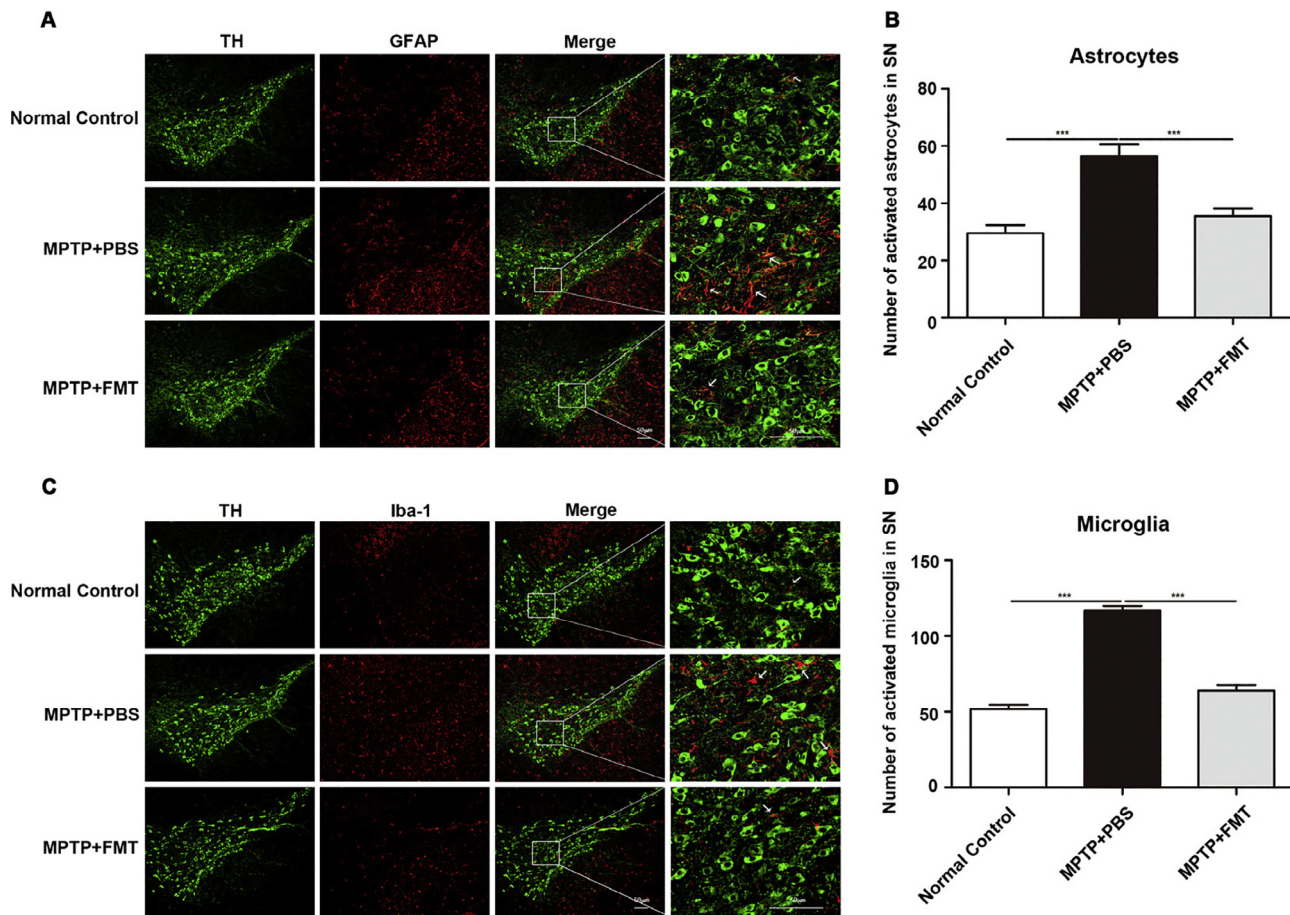


Fig. 6. FMT alleviates microglial and astrocyte activation in the SN of PD mice. (A) Double IF staining for TH, dopaminergic neuron marker; green) and GFAP (astrocyte marker; red) in the SN. The white arrows indicated the GFAP-positive astrocytes in SN. Scale bar is 50 μ m. (B) Quantitative analysis of the number of activated astrocytes in each group. Activation of astrocytes in the SN was lower in the MPTP + FMT group compared to the MPTP + PBS group. (C) Double IF staining of TH and Iba-1 (microglia marker; red) in the SN. The white arrows indicated the IBA-1-positive microglia in SN. Scale bar is 50 μ m. (D) Quantitative analysis of the number of activated microglia in each group, and activation of microglia in the SN was inhibited in the MPTP + FMT group compared to the MPTP + PBS group. Statistical comparison by one-way ANOVA with post hoc comparisons of LSD. Data represent the means \pm s.e.m.; *** p < 0.001. n = 6 mice per group.

activated microglia decreased by 45.3% compared with MPTP + PBS mice (p < 0.001 vs. the MPTP + PBS group) (Fig. 6C and D).

3.6. FMT alleviates gut inflammation and neuroinflammation possibly by suppressing TLR4/TBK1/NF- κ B/TNF- α signaling pathway

To further explore the molecular interactions between gut microbial dysbiosis and neuroinflammation in PD, we characterized colonic and striatal expression of TLR4, TBK1 and NF- κ B by western blot, and TNF- α by ELISA. First, we observed the expressions were higher by 112.1%, 98.1%, 82.6% and 38.2% of TLR4, TBK1 and NF- κ B, as well as TNF- α in the colon of MPTP + PBS mice (p < 0.01, p < 0.01, p < 0.05 and p < 0.05 vs. normal controls, respectively), whereas MPTP + FMT mice displayed decreased expressions of TLR4, TBK1 and NF- κ B, as well as TNF- α by 40.0%, 31.6%, 45.5% and 37.5% in the colon compared with MPTP + PBS mice (p < 0.05, p < 0.05, p < 0.05 and p < 0.01 vs. MPTP + PBS group, respectively) (Fig. 7A–E).

To verify the bidirectional communication between gut and brain, we also showed that TLR4/TBK1/NF- κ B pathway was involved in brain neuroinflammation. Significantly, striatal TLR4, TBK1, NF- κ B and TNF- α expressions were higher by 111.9%, 270.0%, 72.8% and 12.4% in MPTP + PBS mice (p < 0.01, p < 0.01, p < 0.05 and p < 0.05 vs. normal controls, respectively), while MPTP + FMT mice displayed decreased expressions of TLR4, TBK1,

NF- κ B and TNF- α by 52.2%, 64.7%, 38.6% and 16.9% in the striatum compared with MPTP + PBS mice (p < 0.01, p < 0.01, p < 0.05 and p < 0.01 vs. the MPTP + PBS group, respectively) (Fig. 7G–J). In summary, these results suggest that the TLR4/TBK1/NF- κ B/TNF- α signaling pathway is involved in gut inflammation and neuroinflammation, and further that FMT may improve gut microbial dysbiosis to alleviate gut inflammation and neuroinflammation by suppressing this signaling pathway.

4. Discussion

Given the recent evidence that gut microbial dysbiosis occurs in PD patients (Bedarf et al., 2017; Hill-Burns et al., 2017; Li et al., 2017), we also verified the composition differences of gut microbiota in a murine model of PD. Strikingly, our demonstration that gut microbial dysbiosis in PD mice involves decreases in phylum *Firmicutes* and order *Clostridiales*, and increases in phylum *Proteobacteria*, order *Turicibacterales* and *Enterobacteriales*, is consistent with observations in human subjects with PD, which have shown increased abundance of *Proteobacteria* (Keshavarzian et al., 2015; Unger et al., 2016) and *Enterobacteriales* (Unger et al., 2016). It is known that increases in *proteobacteria* can be a consequence of gut inflammation (Nagalingam et al., 2011). In particular, the abundance of *Enterobacteriaceae* has proven to be positively related to the severity of postural instability & gait difficulty

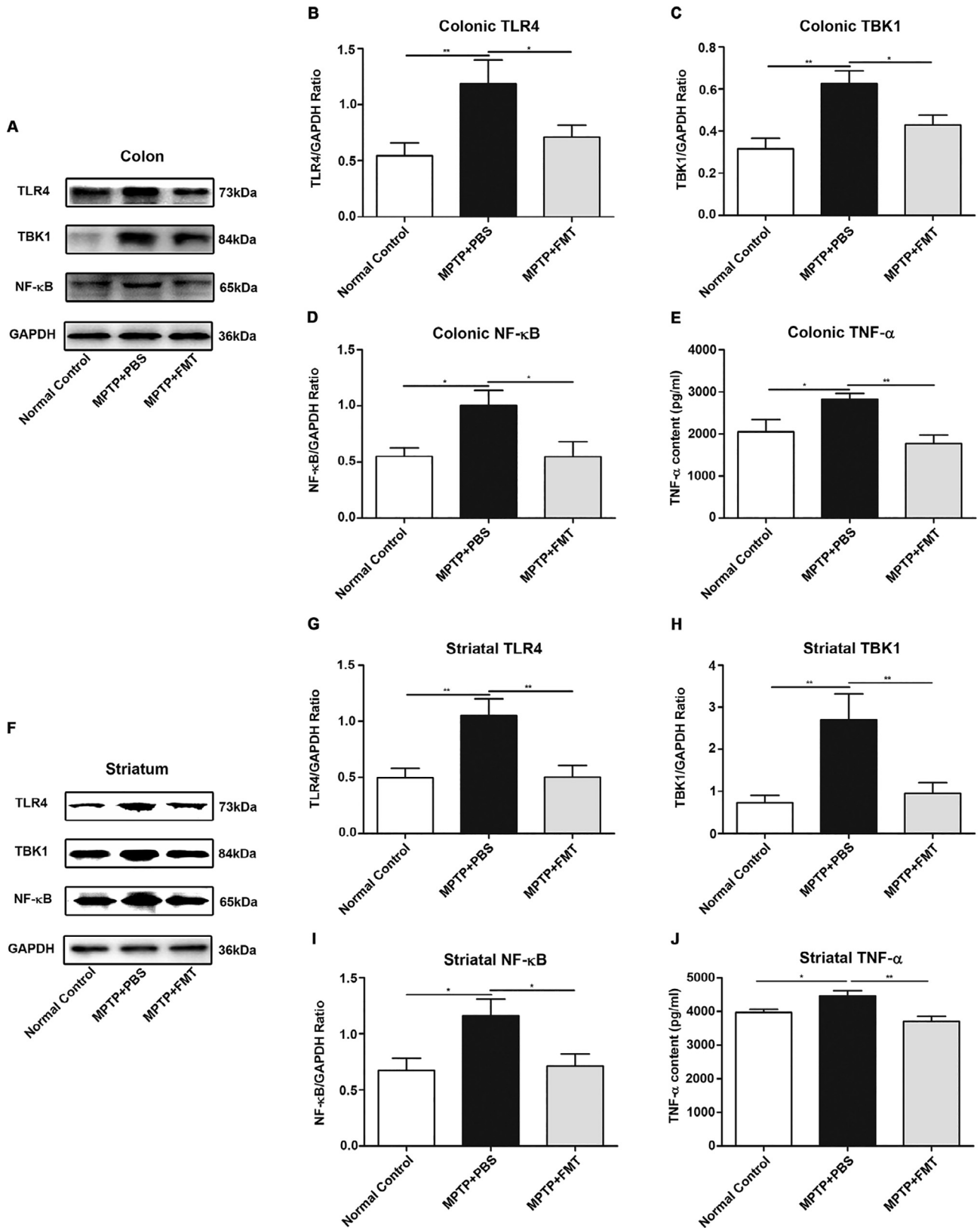


Fig. 7. FMT alleviates gut inflammation and neuroinflammation by suppressing the TLR4/TBK1/NF-κB/TNF-α signaling pathway. (A) Representative western blot of colonic TLR4, TBK1 and NF-κB expression. (B) MPTP-induced high expression of colonic TLR4 was inhibited by FMT. (C) MPTP-induced high expression of colonic TBK1 was inhibited by FMT. (D) MPTP-induced high expression of colonic NF-κB was inhibited by FMT. (E) MPTP-induced high expression of colonic TNF-α was inhibited by FMT. TNF-α expression was quantified by ELISA. (F) Representative western blot of striatal TLR4, TBK1 and NF-κB expression. (G) MPTP-induced high expression of striatal TLR4 was inhibited by FMT. (H) MPTP-induced high expression of striatal TBK1 was inhibited by FMT. (I) MPTP-induced high expression of striatal NF-κB was inhibited by FMT. (J) ELISA analysis of striatal TNF-α expression. MPTP-induced high expression of striatal TNF-α was inhibited by FMT. Statistical comparison by one-way ANOVA with post hoc comparisons of LSD. Data represent the means ± s.e.m.; **P* < 0.05, ***P* < 0.01. n = 6–8 mice. For all western blot results, intensity of bands was quantified with Image J software, and band intensities were normalized to GAPDH.

in PD (Scheperjans et al., 2015), a correlation also shown by our mouse model. These results suggest that gut microbial dysbiosis involving specific microbes may be involved in PD pathogenesis and clinical manifestations.

Recently, the critical role of gut microbiota and microbial metabolites in PD pathogenesis has received increasing attention (Houser and Tansey, 2017). We use PD model by systemic administration of the neurotoxin MPTP to explore the potential role of gut microbiota in PD. After crossing the blood brain barrier, MPTP is converted into its active metabolite MPP⁺ in glial cells by the enzyme monoamine oxidase B (MAO-B). MPP⁺ enters dopaminergic neurons through dopamine transporter (DAT) where it binds to complex I and impairs mitochondrial function. This stimulates the overproduction of free radicals which causes oxidative stress and ultimately leads to the activation of the cell death pathways (Dauer and Przedborski, 2003). Here, we show that gut microbiota from PD mice induces a hallmark of PD motor dysfunctions and neurotransmitter loss in healthy mice. This suggests that gut microbiota not only affects motor symptoms, but also brain function in PD. Consistent with a previous study showing that gut microbiota from PD patients promotes enhanced motor impairment in mice (Sampson et al., 2016), our results show that mice receiving gut microbiota from PD mice also display motor dysfunctions as well as decreases of striatal neurotransmitters. Levels of DA and the DA metabolite DOPAC as well as 5-HT and 5-HIAA are decreased in NS + PD-FMT mice, indicating that PD gut microbiota, but normal gut microbiota impacts brain neurotransmitters expressions. Conversely, PD mice, receiving fecal microbiota from normal mice, display significant recovery of DA, 5-HT and their metabolites in striatum, along with recovery of motor function. DA is an important neurotransmitter responsible for regulating balance and movement, and the perturbations of DA signaling are implicated in the pathogenesis or exploited in the treatment of PD (Tritsch and Sabatini, 2012). Our results indicate that gut microbiota can influence striatal DA concentration and FMT can suppress the loss of dopaminergic neurons in SN. 5-HT is a key neurotransmitter and signaling molecule in the regulation of mood at the level of the CNS and has been implicated in visceral hypersensitivity in the GI tract (Mayer, 2011). It has been reported that gut microbiota constantly controls tryptophan metabolism of the host by kynurenine pathway, thereby simultaneously reducing the fraction available for serotonin synthesis and increasing the production of neuroactive metabolites (Heijtza et al., 2011; O'Mahony et al., 2015). Consistent with this, our data indicate that gut microbiota from PD promotes a decrease in striatal 5-HT concentration. The cross talk of serotonergic system between the gut and brain might explain these differences.

Currently, there are no ideal therapies for PD. Based on the gut microbial dysbiosis in PD patients and mice, our data suggest that reducing gut microbial dysbiosis by FMT has a neuroprotective effect on PD. With a view to manipulate gut microbiota-host interactions, FMT is an exciting potential strategy not only for application in GI disease, such as *Clostridium difficile* infection (CDI) (Konturek et al., 2016) and inflammatory bowel disease (IBD) (Cammarota et al., 2016), but also for the treatment of CNS diseases, such as autism spectrum disorders (ASD) (Kang et al., 2017). Intriguingly, in our study, FMT not only alleviates motor impairment of PD mice, but also improves the dominant microbial population in PD mice, such as phylum *Firmicutes* and order *Clostridiales*. Moreover, we show FMT can rescue the decreases of striatal TH, DA, 5-HT and their metabolites, that occur in PD, while FMT has no side effect on behavioral functions and neurotransmitters on normal mice. These results suggest that FMT exerts a neuroprotective effect by improving gut microbial dysbiosis, resulting in reduced motor impairment and elevated of DA levels, and reduced loss of dopaminergic neurons, as well as restoration of

5-HT synthesis. In previous studies, after FMT, the microbes in recipients were able to be accurately identified for 3–6 months even up to 2 years (Kumar et al., 2017). As a novel treatment, the safety and efficacy of FMT has been proved in CDI patients and there were no other severe adverse events directly attributable to FMT (Hefazi et al., 2017). However, other potential effects of FMT on PD mice should be explored more.

How gut microbial dysbiosis contributes to PD is not clear. Among the potential factors regulating the microbiota-gut-brain axis, microbial SCFAs may be one of major mediators. The study has revealed that differences in fecal SCFA ratios between PD patients and healthy controls, including elevated relative concentrations of butyrate consistent with the observed altered compositions of gut microbiota, implicate a potential role between SCFAs and gut microbiota in PD (Unger et al., 2016). In addition, SCFAs have been recognized as potential mediators of gut microbiota on intestinal immune function and regulation of inflammation (Vinolo et al., 2011). SCFAs are not only trafficked into the serum, but also are capable of crossing the blood brain barrier (BBB) via monocarboxylate transporters to impact the physiology of cells in the CNS such as maturation of microglia, for which mice deficient for the SCFA receptor FFAR2 mirrored microglia defects found under GF conditions (Braniste et al., 2014; Mitchell et al., 2011; Vijay and Morris, 2014). While being fed a mixture of acetate, propionate and butyrate, the three most abundant SCFAs, PD mice display aggravated α -Syn-mediated neuroinflammation, including activation of microglia and motor symptoms (Sampson et al., 2016), suggesting a link between SCFAs and microglia-mediated neuroinflammation. Activation of microglia and astrocytes is responsible for progressive inflammation and neuronal cell death, giving rise to further inflammation and neurodegeneration in the SN-striatum system (Booth et al., 2017; Depboylu et al., 2012; Dutta et al., 2012). Our study also demonstrates that the higher fecal SCFAs concentrations, in PD mice, correlates with higher levels of activated striatal glia, including microglia and astrocytes. Conversely, we observe a lower content of fecal SCFAs along with the lower activation of microglia and astrocytes in the SN of MPTP + FMT mice, compared with MPTP + PBS mice. The above-mentioned studies suggest that fecal SCFAs may contribute to the over activation of microglia and astrocytes in the SN, and FMT may exert a neuroprotective effect via suppression of glia cell activation and lowered expression of fecal SCFAs.

Alterations in gut microbiota have been previously suggested, in Gulf War illness, to activate TLR4, in the small intestine and brain, to explain the intestinal inflammation and neuroinflammation observed (Alhasson et al., 2017). Furthermore, TLR4 deficiency was proved to attenuate up-regulation of AP-1 in TH-positive neurons and astrocytes in the SN of MPTP-treated TLR4-KO mice, which suggested that TLR4 pathway may play an important role in PD pathogenesis (Zhao et al., 2016). Microbial dysbiosis in the gut may result in a leaky gut and release of microbial toxins, such as LPS, into the circulation, ultimately reaching the brain, to impact neurological function. *Proteobacteria*, shown here to be increased in PD mice, is a major gram-negative phylum in mice (Cheng et al., 2013), and is comprised of bacteria with LPS as the major cell wall component, potentially serving as a cause of neuroinflammation through activation of TLR4, and concomitant upregulation of costimulatory signals and cytokines secretion (De Smedt et al., 1996). Our demonstration of FMT-mediated decreases in expression of TNF- α , TLR4, TBK1, and NF- κ B support a close relationship between gut microbial dysbiosis and TLR4/TBK1/NF- κ B/TNF- α signaling pathway-mediated gut inflammation, as well as neuroinflammation, in the pathogenesis of PD. In addition, there might be other potentially signaling pathways involved in gut microbial dysbiosis and neuroprotective effects of FMT on MPTP-induced PD mice. For example, MYD88 is a central adaptor for signaling

through most TLRs especially TLR4, as well as the IL-1 and IL-18 receptors, and disruption of this protein leads to profound innate immune dysfunction response to microbial infection (Rakoff-Nahoum et al., 2004). Furthermore, innate immune cells detect pathogenic and commensal bacteria not only via a TLRs but also NOD-like receptors (NLRs) that are linked to NF- κ B activation, inflammasome assembly, and epithelial repair pathways. Ultimately, these inflammatory responses lead to epithelial damage, loss of mucus-secreting goblet cells, and bacterial translocation, which further stimulates the inflammatory response (Elinav et al., 2011).

Multiple mechanisms and pathways through which the brain and gut interact and influence host behavior involve the sympathetic and parasympathetic branches of autonomic nervous system, as well as the neuroendocrine and immune systems (Grenham et al., 2011). Based on the bidirectional communication between gut and brain, the release of pro-inflammatory factors, such as TNF- α through activation of TLR4/TBK1/NF- κ B signaling pathway in the gut may induce gut immune cells activation which may release some inflammatory factors and then cross BBB to brain glia cells to cause neuroinflammation. Taken together, our findings establish that gut microbial dysbiosis is involved in the pathogenesis of PD, via the microbiota-gut-brain axis, whereby the gut microbiota in PD mice releases microbial components that impact gut inflammation and neuroinflammation. Further, we demonstrate that FMT can reverse gut microbial dysbiosis and result in neuroprotection, possibly by reducing activation of brain glia through lowering activity of the TLR4/TBK1/NF- κ B/TNF- α signaling pathway in both gut and brain. Future studies may also reveal additional molecular markers that could be combined with gut microbial dysbiosis information to enhance the sensitivity and specificity of PD diagnostic assays.

Acknowledgments

This study was supported by National Natural Science Foundation of China – China (81650007, 81771384), Jiangsu Double Innovation Plan of China – China (2014–27), Fundamental Research Funds for the Central Universities of China – China (JUSRP51619B) and Jiangsu Six Peaks Project of China – China (2013-SWYY-041). We sincerely thank Dr. Stanley Li Lin's careful revision on the manuscript.

Appendix A. Supplementary data

Supplementary data associated with this article can be found, in the online version, at <https://doi.org/10.1016/j.bbi.2018.02.005>.

References

- Abreu, M.T., Vora, P., Faure, E., Thomas, L.S., Arnold, E.T., Arditi, M., 2001. Decreased expression of Toll-like receptor-4 and MD-2 correlates with intestinal epithelial cell protection against dysregulated proinflammatory gene expression in response to bacterial lipopolysaccharide. *J. Immunol.* 167, 1609–1616.
- Ahmed, M., Gwaigri, M., Ghanem, A., 2014. Conventional Chiralpak ID vs. Capillary Chiralpak ID-3 Amylose Tris-(3-Chlorophenylcarbamate)-Based Chiral Stationary Phase Columns for the Enantioselective HPLC Separation of Pharmaceutical Racemates. *Chirality* 26, 677–682.
- Alhasson, F., Das, S., Seth, R., Dattaroy, D., Chandrashekar, V., Ryan, C.N., Chan, L.S., Testerman, T., Burch, J., Hofseth, L.J., Horner, R., Nagarkatti, M., Nagarkatti, P., Lasley, S.M., Chatterjee, S., 2017. Altered gut microbiome in a mouse model of Gulf War Illness causes neuroinflammation and intestinal injury via leaky gut and TLR4 activation. *PLoS One* 12.
- Bedarf, J.R., Hildebrand, F., Coelho, L.P., Sunagawa, S., Bahram, M., Goeser, F., Bork, P., Wullner, U., 2017. Functional implications of microbial and viral gut metagenome changes in early stage L-DOPA-naive Parkinson's disease patients. *Genome Med.* 9.
- Booth, H.D.E., Hirst, W.D., Wade-Martins, R., 2017. The role of astrocyte dysfunction in parkinson's disease pathogenesis. *Trends Neurosci.* 40, 358–370.
- Braniste, V., Al-Asmakh, M., Kowal, C., Anuar, F., Abbaspour, A., Toth, M., Korecka, A., Bakocevic, N., Guan, N.L., Kundu, P., Gulyas, B., Halldin, C., Hulthen, K., Nilsson, H., Hebert, H., Volpe, B.T., Diamond, B., Pettersson, S., 2014. The gut microbiota influences blood-brain barrier permeability in mice. *Sci Transl Med.* 6.
- Cammarota, G., Pecere, S., Lanio, G., Masucci, L., Curro, D., 2016. Principles of DNA-Based gut microbiota assessment and therapeutic efficacy of fecal microbiota transplantation in gastrointestinal diseases. *Dig Dis.* 34, 279–285.
- Cani, P.D., Bibiloni, R., Knauf, C., Neyrinck, A.M., Neyrinck, A.M., Delzenne, N.M., Burcelin, R., 2008. Changes in gut microbiota control metabolic endotoxemia-induced inflammation in high-fat diet-induced obesity and diabetes in mice. *Diabetes* 57, 1470–1481.
- Cao, Q., Qin, L.Y., Huang, F., Wang, X.S., Yang, L., Shi, H.L., Wu, H., Zhang, B.B., Chen, Z. Y., Wu, X.J., 2017. Amentoflavone protects dopaminergic neurons in MPTP-induced Parkinson's disease model mice through PI3K/Akt and ERK signaling pathways. *Toxicol Appl. Pharmacol.* 319, 80–90.
- Caporaso, J.G., Kuczynski, J., Stombaugh, J., Bittinger, K., Bushman, F.D., Costello, E.K., Fierer, N., Pena, A.G., Goodrich, J.K., Gordon, J.I., Huttley, G.A., Kelley, S.T., Knights, D., Koenig, J.E., Ley, R.E., Lozupone, C.A., McDonald, D., Muegge, B.D., Pirrung, M., Reeder, J., Sevinsky, J.R., Turnbaugh, P.J., Walters, W.A., Widmann, J., Yatsunenko, T., Zaneveld, J., Knight, R., 2010. QIIME allows analysis of high-throughput community sequencing data. *Nat. Methods* 7, 335–336.
- Cheng, J., Palva, A.M., de Vos, W.M., Satokari, R., 2013. Contribution of the intestinal microbiota to human health: from birth to 100 years of age. *Curr. Top. Microbiol. Immunol.* 358, 323–346.
- Claesson, M.J., O'Sullivan, O., Wang, Q., Nikkila, J., Marchesi, J.R., Smidt, H., de Vos, W.M., Ross, R.P., O'Toole, P.W., 2009. Comparative analysis of pyrosequencing and a phylogenetic microarray for exploring microbial community structures in the human distal intestine. *PLoS One* 4, e6669.
- Dauer, W., Przedborski, S., 2003. Parkinson's disease: mechanisms and models. *Neuron* 39, 889–909.
- De Smedt, T., Pajak, B., Muraille, E., Lespagnard, L., Heinen, E., De Baetselier, P., Urbain, J., Leo, O., Moser, M., 1996. Regulation of dendritic cell numbers and maturation by lipopolysaccharide in vivo. *J. Exp. Med.* 184, 1413–1424.
- Depboylu, C., Stricker, S., Ghobril, J.P., Oertel, W.H., Priller, J., Höglinger, G.U., 2012. Brain-resident microglia predominate over infiltrating myeloid cells in activation, phagocytosis and interaction with T-lymphocytes in the MPTP mouse model of Parkinson disease. *Exp. Neurol.* 238, 183–191.
- Dutta, G., Barber, D.S., Zhang, P., Doperalski, N.J., Liu, B., 2012. Involvement of dopaminergic neuronal cystatin C in neuronal injury-induced microglial activation and neurotoxicity. *J. Neurochem.* 122, 752–763.
- Edgar, R.C., 2010. Search and clustering orders of magnitude faster than BLAST. *Bioinformatics* 26, 2460–2461.
- Elinav, E., Strowig, T., Kau, A.L., Henao-Mejia, J., Thaiss, C.A., Booth, C.J., Peaper, D.R., Bertin, J., Eisenbarth, S.C., Gordon, J.I., Flavell, R.A., 2011. NLRP6 inflammasome regulates colonic microbial ecology and risk for colitis. *Cell* 145, 745–757.
- Evrensel, A., Ceylan, M.E., 2016. Fecal microbiota transplantation and its usage in neuropsychiatric disorders. *Clin. Psychopharmacol. Neurosci.* 14, 231–237.
- Goldstein, D.S., Sewell, L., Sharabi, Y., 2011. Autonomic dysfunction in PD: a window to early detection? *J. Neurol. Sci.* 310, 118–122.
- Grenham, S., Clarke, G., Cryan, J.F., Dinan, T.G., 2011. Brain-gut-microbe communication in health and disease. *Front. Physiol.* 2, 94.
- Guo, H., Shi, F., Li, M.J., Liu, Q.Q., Yu, B., Hu, L.M., 2015. Neuroprotective effects of *Eucommia ulmoides* Oliv. and its bioactive constituent work via ameliorating the ubiquitin-proteasome system. *BMC Complement Altern. Med.* 15.
- Hamilton, M.J., Weingarden, A.R., Sadowsky, M.J., Khoruts, A., 2012. Standardized frozen preparation for transplantation of fecal microbiota for recurrent *Clostridium difficile* infection. *Am. J. Gastroenterol.* 107, 761–767.
- Hefazi, M., Patnaik, M.M., Hogan, W.J., Litzow, M.R., Pardi, D.S., Khanna, S., 2017. Safety and efficacy of fecal microbiota transplant for recurrent *Clostridium difficile* infection in patients with cancer treated with cytotoxic chemotherapy: a single-institution retrospective case series. *Mayo Clin. Proc.* 92, 1617–1624.
- Heijtza, R.D., Wang, S.G., Anuar, F., Qian, Y., Bjorkholm, B., Samuelsson, A., Hibberd, M.L., Forsberg, H., Pettersson, S., 2011. Normal gut microbiota modulates brain development and behavior. *Proc. Natl. Acad. Sci. U.S.A.* 108, 3047–3052.
- Hill-Burns, E.M., Debelius, J.W., Morton, J.T., Wiseman, W.T., Lewis, M.R., Wallen, Z.D., Peddada, S.D., Factor, S.A., Molho, E., Zabetian, C.P., Knight, R., Payami, H., 2017. Parkinson's disease and parkinson's disease medications have distinct signatures of the gut microbiome. *Mov. Disord.* 32, 739–749.
- Houser, M.C., Tansey, M.G., 2017. The gut-brain axis: is intestinal inflammation a silent driver of Parkinson's disease pathogenesis? *NPJ. Parkinsons. Dis.* 3, 3.
- Jankovic, J., 2008. Parkinson's disease: clinical features and diagnosis. *J. Neurol. Neurosurg. Psychiatry* 79, 368–376.
- Kang, D.W., Adams, J.B., Gregory, A.C., Borody, T., Chittick, L., Fasano, A., Khoruts, A., Geis, E., Maldonado, J., McDonough-Means, S., Pollard, E.L., Raux, S., Sadowsky, M.J., Lipson, K.S., Sullivan, M.B., Caporaso, J.G., Krajmalnik-Brown, R., 2017. Microbiota Transfer Therapy alters gut ecosystem and improves gastrointestinal and autism symptoms: an open-label study. *Microbiome* 5, 10.
- Keshavarzian, A., Green, S.J., Engen, P.A., Voigt, R.M., Naqib, A., Forsyth, C.B., Mutlu, E., Shannon, K.M., 2015. Colonic bacterial composition in Parkinson's disease. *Mov. Disord.* 30, 1351–1360.
- Khoruts, A., Weingarden, A.R., 2014. Emergence of fecal microbiota transplantation as an approach to repair disrupted microbial gut ecology. *Immunol. Lett.* 162, 77–81.
- Kim, J.S., Sung, H.Y., 2015. Gastrointestinal autonomic dysfunction in patients with parkinson's disease. *J. Mov. Disord.* 8, 76–82.

- Klindworth, A., Pruesse, E., Schweer, T., Peplis, J., Quast, C., Horn, M., Glockner, F.O., 2013. Evaluation of general 16S ribosomal RNA gene PCR primers for classical and next-generation sequencing-based diversity studies. *Nucl. Acids Res.* 41, e1.
- Konturek, P.C., Koziel, J., Dieterich, W., Haziri, D., Wirtz, S., Glowczyk, I., Konturek, K., Neurath, M.F., Zopf, Y., 2016. Successful therapy of clostridium difficile infection with fecal microbiota transplantation. *J. Physiol. Pharmacol.* 67, 859–866.
- Kumar, R., Yi, N.J., Zhi, D.G., Eipers, P., Goldsmith, K.T., Dixon, P., Crossman, D.K., Crowley, M.R., Lefkowitz, E.J., Rodriguez, J.M., Morrow, C.D., 2017. Identification of donor microbe species that colonize and persist long term in the recipient after fecal transplant for recurrent Clostridium difficile. *NPJ Biofilms Microbi.* 3 (12), 3.
- Kuribara, H., Higuchi, Y., Tadokoro, S., 1977. Effects of central depressants on rotarod and traction performances in mice. *Jpn. J. Pharmacol.* 27, 117–126.
- Li, W., Wu, X., Hu, X., Wang, T., Liang, S., Duan, Y., Jin, F., Qin, B., 2017. Structural changes of gut microbiota in Parkinson's disease and its correlation with clinical features. *Sci. China Life Sci.*
- Lozupone, C., Knight, R., 2005. UniFrac: a new phylogenetic method for comparing microbial communities. *Appl. Environ. Microbiol.* 71, 8228–8235.
- Magoc, T., Salzberg, S.L., 2011. FLASH: fast length adjustment of short reads to improve genome assemblies. *Bioinformatics* 27, 2957–2963.
- Mayer, E.A., 2011. Gut feelings: the emerging biology of gut-brain communication. *Nat. Rev. Neurosci.* 12, 453–466.
- Mitchell, R.W., On, N.H., Del Bigio, M.R., Miller, D.W., Hatch, G.M., 2011. Fatty acid transport protein expression in human brain and potential role in fatty acid transport across human brain microvessel endothelial cells. *J. Neurochem.* 117, 735–746.
- Nagalingam, N.A., Kao, J.Y., Young, V.B., 2011. Microbial ecology of the murine gut associated with the development of dextran sodium sulfate-induced colitis. *Inflamm. Bowel Dis.* 17, 917–926.
- O'Mahony, S.M., Clarke, G., Borre, Y.E., Dinan, T.G., Cryan, J.F., 2015. Serotonin, tryptophan metabolism and the brain-gut-microbiome axis. *Behav. Brain Res.* 277, 32–48.
- Petrov, V.A., Saltykova, I.V., Zhukova, I.A., Alifirova, V.M., Zhukova, N.G., Dorofeeva, Y.B., Tyakht, A.V., Kovarsky, B.A., Alekseev, D.G., Kostryukova, E.S., Mironova, Y. S., Izhboldina, O.P., Nikitina, M.A., Perevozchikova, T.V., Fait, E.A., Babenko, V.V., Vakhitova, M.T., Govorun, V.M., Sazonov, A.E., 2017. Analysis of gut microbiota in patients with Parkinson's disease. *Bull. Exp. Biol. Med.* 162, 734–737.
- Qin, L.Y., Wu, X.F., Block, M.L., Liu, Y.X., Brees, G.R., Hong, J.S., Knapp, D.J., Crews, F. T., 2007. Systemic LPS causes chronic neuroinflammation and progressive neurodegeneration. *Glia* 55, 453–462.
- Rakoff-Nahoum, S., Paglino, J., Eslami-Varzaneh, F., Edberg, S., Medzhitov, R., 2004. Recognition of commensal microflora by toll-like receptors is required for intestinal homeostasis. *Cell* 118, 229–241.
- Ransohoff, R.M., 2016. How neuroinflammation contributes to neurodegeneration. *Science* 353, 777–783.
- Sampson, T.R., Debelius, J.W., Thron, T., Janssen, S., Shastri, G.G., Ilhan, Z.E., Challis, C., Schretter, C.E., Rocha, S., Gradinaru, V., Chesselet, M.F., Keshavarzian, A., Shannon, K.M., Krajmalnik-Brown, R., Wittung-Stafshede, P., Knight, R., Mazmanian, S.K., 2016. Gut Microbiota regulate motor deficits and neuroinflammation in a model of Parkinson's disease. *Cell* 167 (1469–1480), e1412.
- Scheperjans, F., Aho, V., Pereira, P.A., Koskinen, K., Paulin, L., Pekkonen, E., Haapaniemi, E., Kaakkola, S., Eerola-Rautio, J., Pohja, M., Kinnunen, E., Murros, K., Auvinen, P., 2015. Gut microbiota are related to Parkinson's disease and clinical phenotype. *Mov. Disord.* 30, 350–358.
- Schuijt, T.J., Lankelma, J.M., Scicluna, B.P., e Melo, F.D., Roelofs, J.J.T.H., de Boer, J.D., Hoogendijk, A.J., de Beer, R., de Vos, A., Belzer, C., de Vos, W.M., van der Poll, T., Wiersinga, W.J., 2016. The gut microbiota plays a protective role in the host defence against pneumococcal pneumonia. *Gut* 65, 575–583.
- Tritsch, N.X., Sabatini, B.L., 2012. Dopaminergic modulation of synaptic transmission in cortex and striatum. *Neuron* 76, 33–50.
- Ubeda, C., Bucci, V., Caballero, S., Djukovic, A., Toussaint, N.C., Equinda, M., Lipuma, L., Ling, L.L., Gobourne, A., No, D., Taur, Y., Jenq, R.R., van den Brink, M.R.M., Xavier, J.B., Pamer, E.G., 2013.
- Unger, M.M., Spiegel, J., Dillmann, K.U., Grundmann, D., Philippeit, H., Burmann, J., Fassbender, K., Schwiertz, A., Schafer, K.H., 2016. Short chain fatty acids and gut microbiota differ between patients with Parkinson's disease and age-matched controls. *Parkinsonism Relat. Disord.* 32, 66–72.
- Vijay, N., Morris, M.E., 2014. Role of monocarboxylate transporters in drug delivery to the brain. *Curr. Pharm. Des.* 20, 1487–1498.
- Vinolo, M.A.R., Rodrigues, H.G., Nachbar, R.T., Curi, R., 2011. Regulation of inflammation by short chain fatty acids. *Nutrients* 3, 858–876.
- Wang, Y., Kasper, L.H., 2014. The role of microbiome in central nervous system disorders. *Brain Behav. Immun.* 38, 1–12.
- Zhang, J., Zhu, C., Guan, R., Xiong, Z., Zhang, W., Shi, J., Sheng, Y., Zhu, B., Tu, J., Ge, Q., Chen, T., Lu, Z., 2017. Microbial profiles of a drinking water resource based on different 16S rRNA V regions during a heavy cyanobacterial bloom in Lake Taihu, China. *Environ. Sci. Pollut. Res. Int.* 24, 12796–12808.
- Zhao, L., Wang, G., Siegel, P., He, C., Wang, H., Zhao, W., Zhai, Z., Tian, F., Zhao, J., Zhang, H., Sun, Z., Chen, W., Zhang, Y., Meng, H., 2013. Quantitative genetic background of the host influences gut microbiomes in chickens. *Sci. Rep.* 3, 1163.
- Zhao, X.D., Wang, F.X., Cao, W.F., Zhang, Y.H., Li, Y., 2016. TLR4 signaling mediates AP-1 activation in an MPTP-induced mouse model of Parkinson's disease. *Int. Immunopharmacol.* 32, 96–102.